# Optimizing residential mechanical ventilation against airborne infections: A computational fluid dynamics approach

Fatemeh Keramat[1], Lexuan Zhong[1*]
[1, 1*] Department of Mechanical Engineering, University of Alberta, 9211-116 Street NW, Edmonton, AB T6G1H9, Canada

## Abstract

Ventilation significantly impacts airflow and virus dispersion, emphasizing the need for efficient systems to reduce COVID-19 spread in indoor environments. Research mostly focused on non-residential buildings, with residential ventilation optimization less explored. This study evaluates a typical ventilation system in a British Columbia detached house using Computational Fluid Dynamics (CFD) simulations, assessing its efficacy in minimizing airborne infection risks. Covering eight scenarios, the simulations explore different diffuser locations, furniture arrangements, and positions of infected individuals, incorporating flow, heat, and particle behaviors. Employing the modified Wells-Riley model, which includes ventilation rates and social distancing, the research evaluates infection probabilities, focusing on particle concentrations as an additional risk indicator. Findings reveal that enhanced ventilation and increased social distancing significantly lower infection risks. Moreover, design modifications like adding diffusers and enabling natural convection through windows markedly influence particle distribution and virus spread, achieving the lowest infection risk in the optimally conditioned living room.

## Introduction

The COVID-19 pandemic has emphasized the critical role of indoor air quality in controlling the spread of airborne diseases, with the virus's transmission being notably affected by air circulation in enclosed spaces. Enhancing ventilation is necessary, as highlighted by the World Health Organization, prompting governments to revise HVAC system guidelines for better pandemic preparedness [1, 2].

Epidemiological data emphasize the risk of infection through aerosols generated by normal respiratory activities, which vary significantly in size and emission speed, influencing their airborne persistence and the subsequent infection risk in indoor environments [3-7]. The relationship between ventilation rates and the concentration of infectious particles forms the basis of assessing airborne transmission risks, as demonstrated by the development and adaptation of models like the Wells–Riley equation, which correlates indoor ventilation with infection probability [8, 9]. This foundational understanding has been expanded to consider the impacts of social distancing and enhanced ventilation strategies on minimizing indoor transmission risks, offering crucial insights for designing future anti-infection HVAC systems [9].

Computational Fluid Dynamics (CFD) simulations, including the Large Eddy Simulation (LES) approach, are essential for optimizing ventilation rates to minimize contagion risks while ensuring energy-efficient ventilation systems [10]. These simulations are crucial for understanding aerosol dynamics in various environments. Vuorinen et al. [11] utilized 3D CFD and LES to study aerosol behavior from speaking and coughing, aiming to identify high-risk zones for transmission in public spaces and apply Monte-Carlo Modelling to assess exposure risks in different scenarios [11]. Similarly, Villafruela et al. [12] used CFD to analyze how ventilation designs influence the spread of exhaled contaminants, demonstrating the model's accuracy in predicting airflow and particle distribution in enclosed spaces. Research also extends to the dynamics of droplet spread from coughing and sneezing in both indoor and outdoor settings, with findings significant for respiratory disease transmission mitigation [13, 14].

Additionally, studies have quantified infection risks based on particle number and distribution under various ventilation strategies, highlighting the importance of distance and hygiene measures to reduce transmission risks from cough droplets [15]. For multi-zone infection risk analysis, Yan et al. [16] utilized CONTAM software to model airborne SARS-CoV-2 transmission in a multi-zone office building, assessing various mitigation strategies. They applied the Wells-Riley equation to evaluate infection probabilities across different building zones, highlighting the effectiveness of combined mitigation approaches in reducing transmission risks.

This study investigates various ventilation strategies, which include adjusting the number of diffusers and their locations, as well as opening windows to enhance natural convection within the building. Additionally, the placement of an infected individual within the residential building is examined as another critical parameter using CFD simulations.

## Problem definition

The simulation objective is to analyze COVID-19 transmission within a detached residential building in British Columbia, based on layouts from the BC Housing annual publication [17], which incorporates a detailed environment with three occupants, one of whom is infected. Based on Fig. 1, the house features two bedrooms, a living

room, a kitchen, two washrooms, laundry, and a storage room, complemented by walk-in closets in the bedrooms and three heating baseboards in the living area and bedrooms. Furniture elements include sofas and a coffee table in the living room, two beds in the bedrooms, and essential fixtures like sinks, toilets, and cabinets in the kitchen and washrooms, creating a realistic setting for the simulation. Entrances to each space are considered interior boundaries. Occupants are modeled as cylinders, a simplification for analyzing respiratory particle dynamics, with a focus on particles expelled at a velocity of 4 m/s while speaking. It should be noted that the mouth diameter is assumed 5 cm.

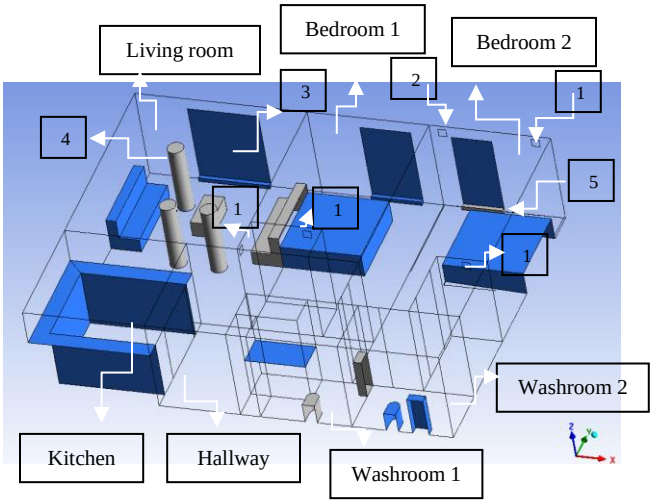


1: Fresh air inlet, 2: Outlet diffuser, 3: Windows, 4: Individuals, 5: baseboards

*Figure 1. Residential building layout indicating different zones, boundaries, and symbolic persons*

**Eight Different Scenarios**

The following scenarios were simulated to explore the impact of various ventilation strategies and people arrangements on air quality and particle spread within a residential setting:

1- **Without Furniture**: This scenario represents a baseline setting where the environment is void of any furniture, providing a clear understanding of airflow without obstructions. The focus is on the natural ventilation patterns within the space, assuming no additional variables introduced by furniture that could impact air circulation and distribution.

2- **Infected Person in the Living Room - Type 1 Ventilation**: In this scenario, an infected individual is present in the living room with type 1 ventilation in place. This type of ventilation involves regular airflow, where both the air inlet and outlet are located in the second bedroom, allowing air to circulate from outside through this room. This setup examines how the presence of an infected person in a common area affects the spread of pathogens with standard ventilation.

3- **Infected in the Bedroom - Type 1 Ventilation**: This scenario places the infected individual in a bedroom, again with type 1 ventilation. The focus is on observing how the pathogens potentially circulate within a more confined space under regular ventilation conditions, where air flows directly from outside through the second bedroom's inlet and outlet.

4- **Infected Person in Bedroom - Type 2 Ventilation**: Here, the infected person is in bedroom 1, but with an additional inlet added to this room, representing type 2 ventilation. This configuration aims to assess the impact of enhanced ventilation in the room with the infected individual by increasing air intake from outside, potentially diluting the concentration of airborne pathogens.

5- **Infected Person in Bedroom - Type 3 Ventilation**: In this adjusted scenario, the infected person is in bedroom one, with type 3 ventilation introducing both an additional air outlet and an inlet diffuser in bedroom one, aiming to improve air exchange and reduce pathogen concentration.

6- **Infected Person in Bedroom - Type 4 Ventilation (Open Window, Inlet Pressure):** This scenario focuses on the effect of natural ventilation through an open window in the bedroom with the infected individual, assessing its impact on air quality and pathogen dispersion, considering the pressure inlet as the window boundary condition.

7- **Infected Person in Bedroom - Type 5 Ventilation (Open Window, Outlet Pressure):**
This scenario examines how natural ventilation from an open bedroom window affects air quality and pathogen spread, considering the window as a pressure outlet boundary condition.

8- **Infected Person in Bedroom - Type 6 Ventilation**
In this type of ventilation setup, the living room and two bedrooms each have mechanical ventilation systems, which include one inlet and one outlet. The infected person still is located in bedroom 1.

**Boundary Conditions**

Table 1 summarizes the boundary conditions used in this study. The mass flow inlet type boundary was defined for all air entering different zones. Additionally, the source of particles exiting from an infected person's mouth is defined by the inlet velocity. For the scenario involving an open window, the air pressure inlet is defined as the inlet boundary type.

*Table 1: Boundary conditions of the ventilation and persons in the domain*

| Boundary type | Boundary condition | Value | DPM |
|---|---|---|---|
| Inlets to the bedrooms and living room | Mass flow inlet | 0.05 kg/s [18] T=298 K | escape |

| Outlet | Pressure outlet | Atmospheric pressure | escape |
|---|---|---|---|
| Walls in different zones | No-slip wall | Heat flux=0 w/m$^2$ | reflect |
| Baseboard's surfaces | No-slip wall | T= 338 K | reflect |
| Furniture surfaces | No-slip wall | Heat flux=0 w/m$^2$ | reflect |
| Person body surfaces | No-slip wall | T= 310 K [12] | reflect |
| Source of particles | Velocity inlet (Infected mouth) | 4 m/s [19] T=310 K | escape |
| Windows | Pressure inlet | P=$P_{atm}$ T=278 K | escape |

## Methodology

This project can be categorized into three steps, including pre-processing, processing, and post-processing. Pre-processing contains the preparation of the geometry in Gambit 2.4.6 software, mesh generation, mesh independence analysis, and validation. Processing is the simulation procedure using ANSYS Fluent 20.0 software, and the post-processing with the CFD-POST software is used for extracting the results.

## Governing Equations

The governing equations refer to the Navier Stokes equations for the mass conservation, momentum, and energy are presented in this section. The K-e turbulent model, Discrete phase model (DPM), and energy model are activated and the relevant equations are indicated as Eq (1) to Eq (5).

Continuity equation [20]:

$$\frac{\partial \rho}{\partial t} + \nabla.(\rho \vec{v}) = 0 \qquad (1)$$

where ρ (kg/m3) is fluid density and v is velocity vector (m/s).

Conservation of momentum equation [20]:

$$\frac{\partial}{\partial t}(\rho \vec{v}) + \nabla.(\rho \vec{v}\vec{v}) = -\nabla p + \nabla.(\bar{\bar{\tau}}) + \rho \vec{g} + \vec{F} \qquad (2)$$

where p is the static pressure (N/m2), τ is the surface shear stress (N/m2), and ρ g is the gravitational body force (N) and F is the external body force (N).

The particle motion equation is also used to calculate each particle trajectory by solving the momentum equation [20].

$$\frac{d\vec{u}_p}{dt} = F_D(\vec{u} - \vec{u}_p) + \frac{\vec{g}(\rho_p - \rho)}{\rho_p} + \vec{F}_a \qquad (3)$$

Turbulent K-e model equation [20]:

$$\frac{\partial(\rho k)}{\partial t} + div(\rho k \vec{v}) = div\left[\frac{\mu_t}{\sigma_k} grad k\right] + 2\mu_t S_k . S_k - \rho\varepsilon \qquad (3)$$

$$\frac{\partial(\rho \varepsilon)}{\partial t} + div(\rho \varepsilon \vec{v}) = div\left[\frac{\mu_t}{\sigma_k} grad \varepsilon\right] + C_{1\varepsilon}\frac{\varepsilon}{K} 2\mu_t S_k . S_k - C_{2\varepsilon}\rho\frac{\varepsilon^2}{K} \qquad (4)$$

$k$ is the turbulent kinetic energy (J/kg); ε is the rate of dissipation of turbulent kinetic energy (m2/s3); $S_k$, $S_\varepsilon$ are the source terms v is the fluid velocity vector; C μ , σ ε, σ k, C1ε, and C2ε are the empirical constants [20].

Energy balance equation [20]:

$$\frac{\partial}{\partial t}(\rho c T)dV = (\lambda\frac{\partial T}{\partial X} + \lambda\frac{\partial T}{\partial Y} + \lambda\frac{\partial T}{\partial Z}).dA \qquad (5)$$

## Numerical approach

All of the cases are simulated using Fluent 20.0 software with double precision solver. The continuity, momentum, energy, turbulent K-e model, and discrete phase model (DPM) are solved to predict the flow, heat, and particle concentration behavior within the system. The mean diameter of exhaled breath COVID-19 particles from an infected person's mouth is assumed to be 0.53 μm and 2.49 μm based on the Edwards study [21]. The particles were injected in a direction perpendicular to the patient's mouth. It should be noted that the decay rate of particles is assumed to be negligible in this study, as the evaporation of particles is not considered.

SIMPLE algorithm is used to join the momentum and mass conservation equations. For the higher accuracy of the convergence and the results, the second-order upwind discretization method is used. Finally, the residual criteria for solving all of the governing equations are selected as $10^{-6}$.

Based on the effective parameters in this study, the modified W–R model presented by Sun and Zhai [9] was used for implementing social distancing and developing ventilation systems to prevent infection, as detailed in Equation (6).

$$P = 1 - \exp(-P_d \frac{Iqpt}{Q.E_z}) \qquad (6)$$

where

$I$ : Number of infectors

t: Exposure time (h) = 8hr

$q$ : number of infected airborne per person per minute = 0.3 m$^3$/h

$p$ : Pulmonary ventilation rate of each susceptible per hour (quanta/h) P=48 [22]

$Q$ : Room ventilation rate m$^3$/hr

$E_z$=1.0 (ASHRAE,2019)

$$P_d = (-18.19\ln(d) + 43.276)/100 \qquad (7)$$

The distance index Pd in eq (7) was calculated through theoretical analysis of how droplets are distributed and transmitted when speaking.

Therefore, the final version of the modified W-R model for this study is obtained as eq (8).

$$P = 1 - \exp(-(-18.19\ln(d) + 43.276)/100)\frac{115.2}{Q}) \quad (8)$$

## Mesh structures and mesh independence test

Figure 2 depicts the mesh structure for the sofa, coffee table, and two persons in the living room, representing the mesh structure across all domains. The tetrahedral volume mesh is applied in all domains, and the boundary layer mesh is applied to the mouths of the symbolic persons. Mesh independence analysis is indicated in Fig. 3. The minimum number of mesh elements that guarantees the independence of the mesh is 14,150,101. The outlet velocity is chosen as a comparative result to determine the optimum number of mesh elements in the simulation.

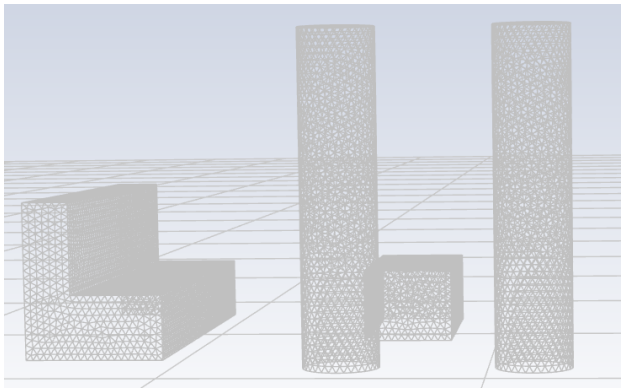

*Figure 2. Mesh structure for the furniture and symbolic persons in the third scenario*

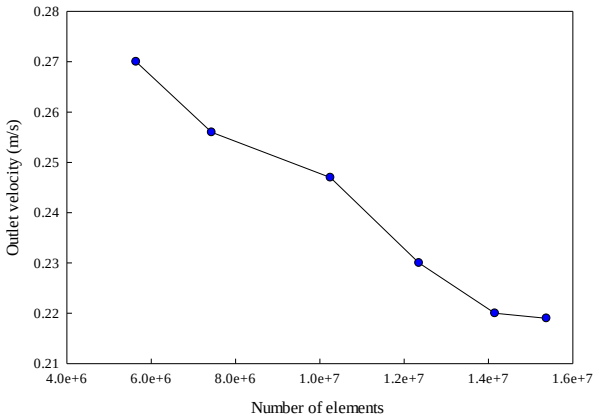


*Figure 3. Mesh independence analysis for the third scenario*

## Validation

This study is validated against [18], focusing on airflow patterns in a room with mechanical ventilation and three people, one infected with COVID-19. This validation aimed to ensure the simulation's accuracy in depicting how air moves and potentially carries the virus in indoor settings. In their study, they used K-e RLZ for the turbulent model simulation. The second-order upwind scheme and SIMPLE algorithm were used for pressure-velocity coupling modeling. Figure 4 shows the airflow patterns from both our current simulation and the previous work, highlighting a strong agreement between them. The maximum air velocity was observed at the airflow inlet diffuser and the right wall in this case.

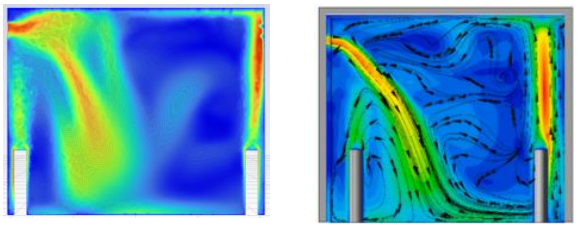

*(a)* *(b)*

*Figure 4. Comparing airflow patterns under mechanical ventilation: (a) current vs. (b) previous study [18]*

## Results and Discussion

### Streamline and velocity distribution

Figure 5 demonstrates the airflow streamline inside the building in different zones. The air velocity varies between 0 to 0.75 m/s, indicating the maximum velocity close to the airflow inlet and outlet boundaries. The fluid behavior and velocity can be indicated by the spacing between every single streamline. The direction of the streamlines indicates the path that fluid elements follow. The patterns also predict the areas where the fluid accelerates, decelerates, or changes direction.

For example, at the inlet boundary in bedroom 2, streamlines are closer together, and the fluid velocity is higher. In the living room, the streamlines diverge, which means flow might be slowing down. The streamlines also reveal how the fluid interacts with the geometry within the volume, including navigation around corners, bends, and objects placed in the flow path.

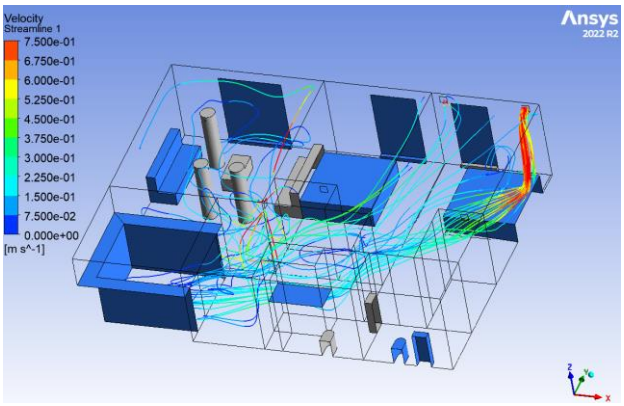


*Figure 5. Airflow streamlines in different zones*

Figure 6 presents the three-dimensional velocity indicating the velocity magnitude and direction of the airflow path in the first, third, sixth (open-window), and eighth scenarios. Compared to the close-window case, the open-window

scenario provides additional ventilation, potentially increasing airflow and creating new paths for air to move through bedroom 1. This might lead to higher velocities and more dispersed distribution, as fresh air enters and mixes with the indoor air. In this case, the pressure dynamics change within the room, which can change the direction and velocity of airflow. The more evenly distributed airflow could be due to this new natural ventilation pathway.

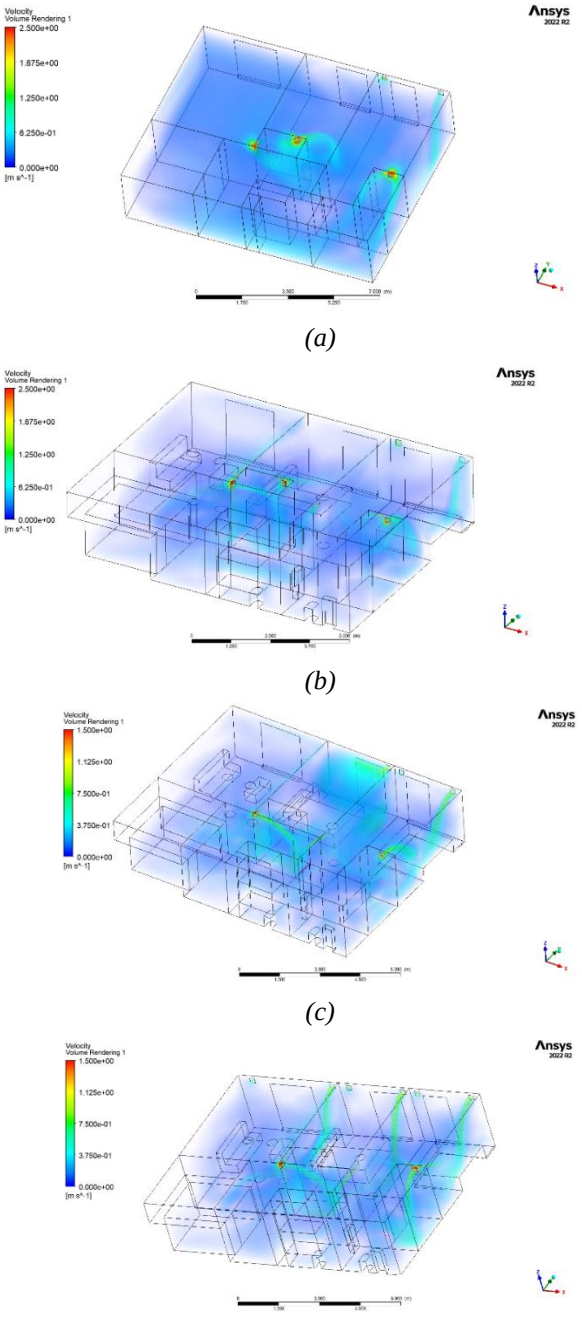


*Figure 6. 3D-velocity of the airflow in the building (a) without furniture, (b) third, (c) sixth (open-window) scenarios, (d) eighth scenario*

**Particle distribution and infection risk evaluation**

Figure 7 indicates the 3D particle concentration distribution in different zones for the third case, where the infected person is in bedroom 1. The right side of the building, including bedroom 2, is where a higher infection risk will happen due to the higher particle concentration. The possibility of infection decreases in the hallway and especially in the living room. This is because of the lower air recirculation on the left side of the building, which carries fewer particles to these places. Conversely, on the right side of the building, where the air inlets and outlet are situated, the chance of particle movement and accumulation increases.

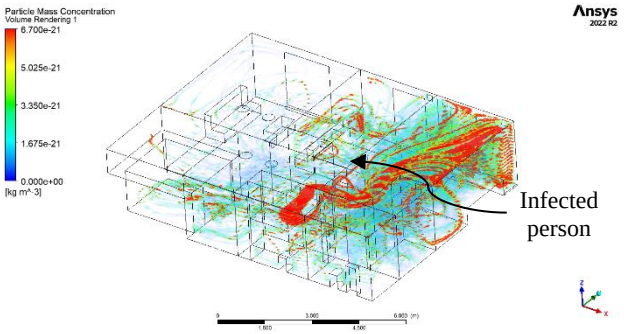


*Figure 7. Particle concentration distribution in different zones: (third case)*

Figure 8 shows the gradient of particle mass concentration from the top view of the building for all scenarios. In addition, the possibilities of infection risk in habitable spaces are presented in Table 2 using Equation (8). According to this equation, the two variables that affect the infection risk in this study are social distance and ventilation rate in each room. Generally, the kitchen, bathrooms, and storage rooms are assumed to be used briefly by the occupants, and thus the infection risk in these areas is considered negligible. In the second scenario, the distances from the infected person to individuals in the living room, bedroom 1, and bedroom 2 are 2.0 m, 2.5 m, and 4.5 m, respectively. For the remaining scenarios, the infected person is located in bedroom 1 with distances of 4.0 m to the living room, 0.5 m to bedroom 2, and 1.0 m to bedroom 3.

It should be mentioned that the first scenario, without an infected person and furniture, is not presented in this section. In general, some regions in the bedroom 1 and 2 are shown with the highest particle mass concentration. These could be locations of particle sources, areas, or regions where particles naturally accumulate due to the flow dynamics. Areas with high concentrations could represent higher infection risks, as there are more potentially infectious particles present.

When all of the individuals are present in the living room (second case), the chance of being infected by viruses in this

place is higher than in other zones in the building. The infection risk percentage also confirms that the living room has a higher potential for infection (21.89%) because the infected person is in the living room. There is a 10% difference in infection risk across different zones. Since the ventilation rates in each zone are approximately the same, social distance is the only factor affecting infection risk.

In the third scenario, there are three airflow inlets and one outlet diffuser. An infected person is located in bedroom 1, and the pathway of the virus, marked by a high concentration, begins at the injection source (the mouth of the infected person). After recirculating in a small part of the hallway, it moves toward the outlet diffuser in bedroom 2. The other areas affected by the infection are the hallway and the kitchen. The highest infection risk possibility occurs in bedrooms 1 and 2, with 35.66% and 29.26% respectively. The living room can be considered a safer place, with a 13.34% infection risk in this scenario, due to the lower virus concentration and greater distance from the infected person.

Regarding the fourth scenario, this configuration aims to assess the impact of additional ventilation in the room with the infected individual by increasing air intake from outside, potentially diluting the concentration of airborne pathogens. However, more ventilation in this room increases the air recirculation and causes higher concentration particles in this zone compared to the third scenario. That's why the highest infection risk occurs in bedroom 2 (63.1 %) in this case. In the fifth scenario, there are inlet and outlet diffusers in bedroom 1. The presence of the outlet diffuser in the bedroom redistributes particles in this zone. Additionally, particles tend to recirculate in the living room and Bedroom 2 as well. Therefore, bedroom 2 remains a riskier location than the living room, following bedroom 1.

For the open-window case with inlet pressure (6th scenario), the volume rendering shows a complex pattern of particle distribution, which is likely influenced by the introduction of outdoor air through the open window. It should be noted that the infected person is in the same bedroom with an open window, exposing individuals to infection risks of 24.19% in bedroom 2 and 13.34% in the living room, respectively. Additionally, higher levels of fresh air help to reduce the infection risk in bedroom 1 compared to the third and fifth scenarios. In the 7th scenario, natural convection is introduced into the building through the outlet pressure. In this case, the pressure difference causes air containing infected particles to move toward the open window. Consequently, the other zones in the building remain clear of particles, which highlights the positive effect of natural ventilation. This is especially true in indoor environments where the pressure is lower than outdoors, directing particles outside. However, based on infection risk analysis, the possibility of infections still exists in this case.

In the 8th scenario, where the living room and bedrooms each have their ventilation systems (comprising diffusers and outlets), particles are likely to disperse throughout the entire building. This distribution occurs due to the high level of airflow recirculation, which results from the addition of two sets of diffusers and outlets to the building. In this case, the infection risk is minimized in the living room (6.91%) compared to all of the scenarios.

*Table 2. Infection risk across different zones in all scenarios*

| scenario | Living room | Bedroom 1 | Bedroom 2 |
|---|---|---|---|
| 2nd | 21.89% | 18.94% | 11.96% |
| 3rd | 13.34% | 35.66% | 29.26% |
| 4th | 13.34% | 19.79% | 63.10% |
| 5th | 13.34% | 38.37% | 33.11% |
| 6th | 13.34% | 27.06% | 24.19% |
| 7th | 13.34% | 29.52% | 26.08% |
| 8th | 6.91% | 35.66% | 15.70% |

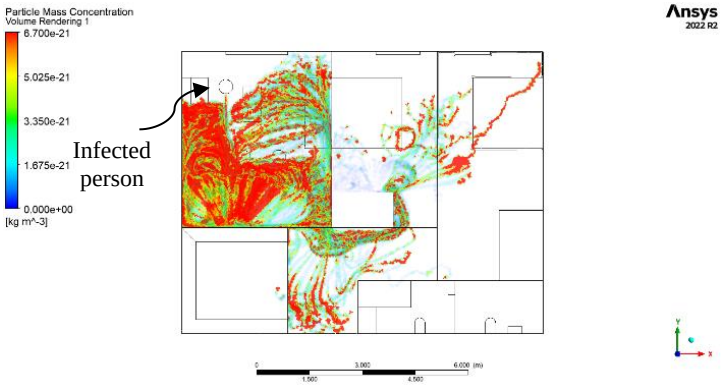


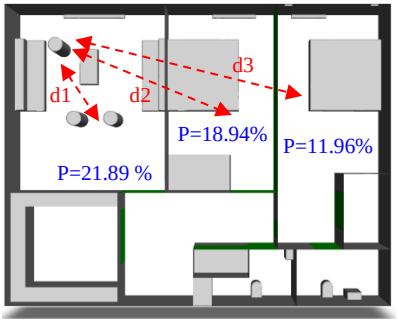


d1=2.0 m
d2=2.50 m
d3=4.50 m
$Q_{living\ room}$=146 $m^3/hr$
$Q_{bedroom\ 1}$=146 $m^3/hr$
$Q_{bedroom\ 2}$=144 $m^3/hr$

*2nd scenario*

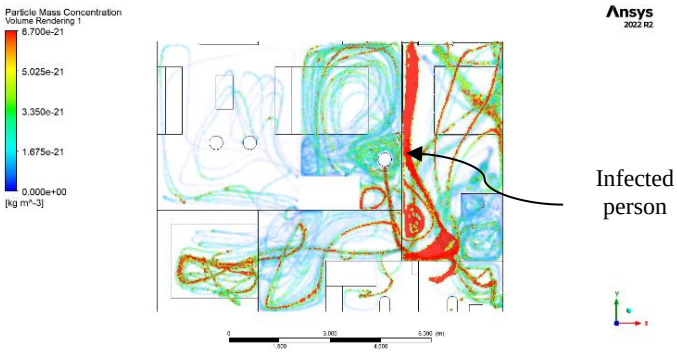

d1=4.0 m
d2=0.50 m
d3=1.00 m
$Q_{living\ room}$=146 $m^3$/hr
$Q_{bedroom\ 1}$=146 $m^3$/hr
$Q_{bedroom\ 2}$=144 $m^3$/hr

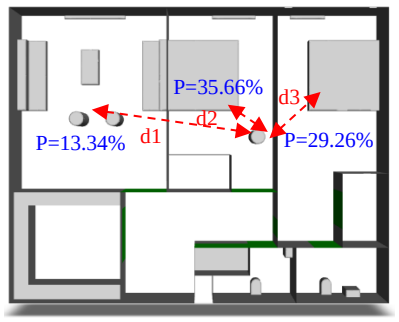


*3rd scenario*

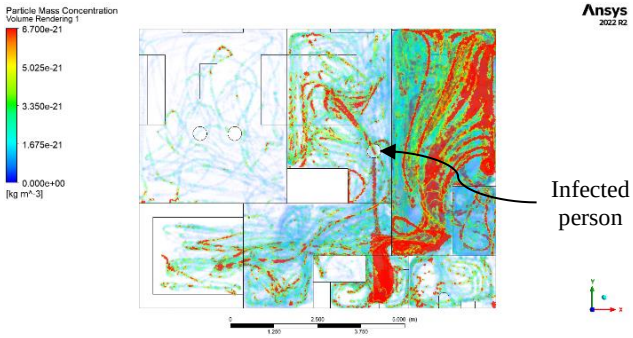


*4th scenario*

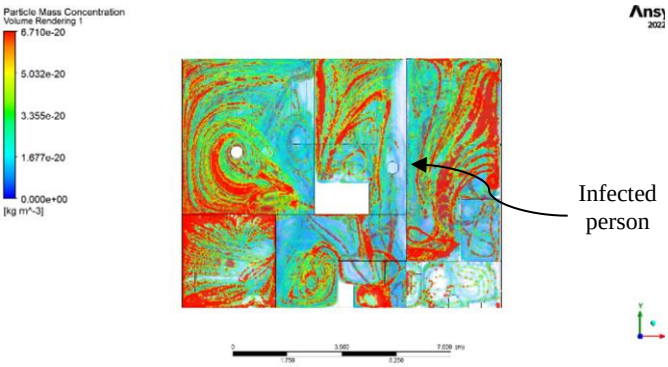


*5th scenario*

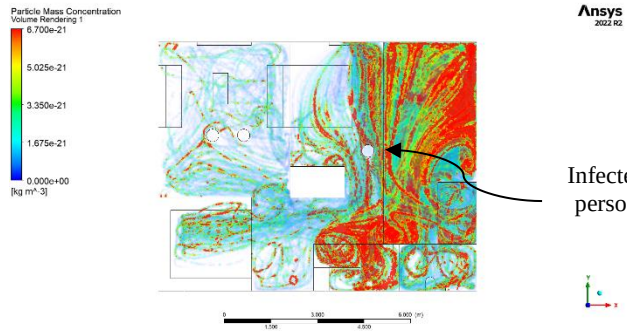


*6th scenario (open window, inlet pressure)*

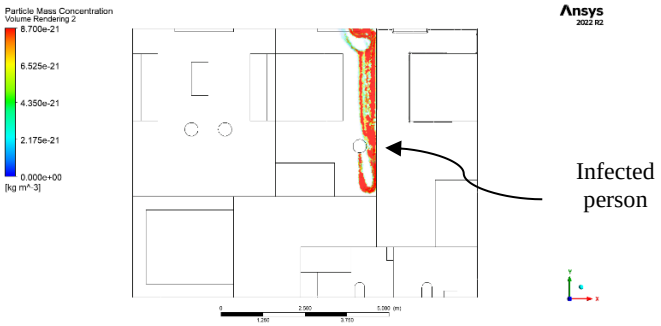


*7th scenario (open window, outlet pressure)*

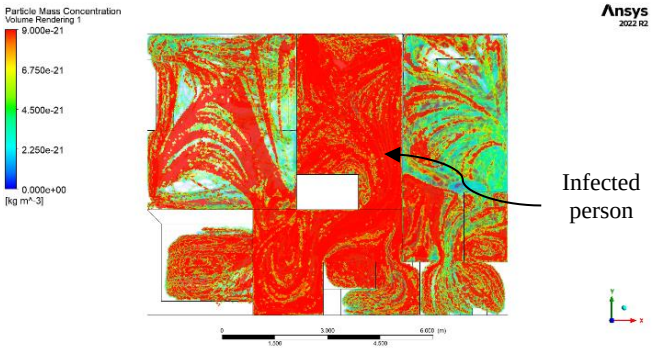


*8th scenario*

*Figure 8. Particle concentration distribution and infection risk % for different zones in different scenarios*

## Conclusion

In this study, the CFD simulation of a residential building including multiple zones to find the fluid and particle behavior produced by an infected person was performed. The results show:

- Air velocity inside the building varies from 0 to 0.75 m/s, with streamline spacing indicating fluid behavior and directional flow, particularly noting higher velocities near inlets and outlets.
- The introduction of open windows using inlet pressure enhances airflow and distribution, with changes in pressure dynamics leading to more dispersed and higher air velocities, especially through bedroom 1.
- On the other hand, by applying the pressure outlet boundary to the window, the particles disappear from the other zones and move towards the window to exit. Although the particles are less concentrated in this case, the infection risk still exists based on the modified W-R model.
- Scenario analysis indicates that the presence of individuals in the living room increases infection risk there due to lower ventilation. However, in scenarios with targeted ventilation strategies, like opening windows or adding air inlets, airflow patterns and particle distribution vary.

- Enhanced ventilation, either through increased air intake or opening windows influences air recirculation and particle distribution patterns, affecting infection risk dynamics across different zones within the building, which is more likely to happen in reality.
- The minimum infection risk occurs in the living room in the 8th scenario where all of the habitable spaces have their own fresh air inlet and air exhaust.

## Acknowledgment

The authors gratefully acknowledge the funding provided by BC Housing through Building Excellence Research & Education Grant.

## References

1. 2021 [cited 2024 January 23]; Available from: https://www.who.int/news-room/questions-and-answers/item/coronavirus-disease-covid-19-ventilation-and-air-conditioning.
2. Zheng, W., et al., *COVID-19 impact on operation and energy consumption of heating, ventilation and air-conditioning (HVAC) systems.* Advances in Applied Energy, 2021. **3**: p. 100040.
3. Wiersinga, W.J., et al., *Pathophysiology, transmission, diagnosis, and treatment of coronavirus disease 2019 (COVID-19): a review.* Jama, 2020. **324**(8): p. 782-793.
4. Shao, S., et al., *Risk assessment of airborne transmission of COVID-19 by asymptomatic individuals under different practical settings.* Journal of aerosol science, 2021. **151**: p. 105661.
5. Rudnick, S. and D.K. Milton, *Risk of indoor airborne infection transmission estimated from carbon dioxide concentration.* Indoor air, 2003. **13**(3): p. 237-245.
6. Lindsley, W.G., et al., *Quantity and size distribution of cough-generated aerosol particles produced by influenza patients during and after illness.* Journal of occupational and environmental hygiene, 2012. **9**(7): p. 443-449.
7. Duguid, J., *The size and the duration of air-carriage of respiratory droplets and droplet-nuclei.* Epidemiology & Infection, 1946. **44**(6): p. 471-479.
8. Riley, E., G. Murphy, and R. Riley, *Airborne spread of measles in a suburban elementary school.* American journal of epidemiology, 1978. **107**(5): p. 421-432.
9. Sun, C. and Z. Zhai, *The efficacy of social distance and ventilation effectiveness in preventing COVID-19 transmission.* Sustainable cities and society, 2020. **62**: p. 102390.
10. Ferrari, S., et al., *Ventilation strategies to reduce airborne transmission of viruses in classrooms: A systematic review of scientific literature.* Building and Environment, 2022: p. 109366.
11. Vuorinen, V., et al., *Modelling aerosol transport and virus exposure with numerical simulations in relation to SARS-CoV-2 transmission by inhalation indoors.* Safety science, 2020. **130**: p. 104866.
12. Villafruela, J., et al., *CFD analysis of the human exhalation flow using different boundary conditions and ventilation strategies.* Building and Environment, 2013. **62**: p. 191-200.
13. Kotb, H. and E.E. Khalil. *Impact of sneezed and coughed droplets produced from a moving passenger on other passengers inside aircraft cabins*. in *AIAA Propulsion and Energy 2020 Forum*. 2020.
14. Li, H., et al., *Dispersion of evaporating cough droplets in tropical outdoor environment.* Physics of Fluids, 2020. **32**(11).
15. Li, H., K. Zhong, and Z.J. Zhai, *Investigating the influences of ventilation on the fate of particles generated by patient and medical staff in operating room.* Building and Environment, 2020. **180**: p. 107038.
16. Yan, S., et al., *Evaluating SARS-CoV-2 airborne quanta transmission and exposure risk in a mechanically ventilated multizone office building.* Building and Environment, 2022. **219**: p. 109184.
17. Housing, B., *Building Enclosure Design Guide Wood-Frame Multi-Unit Residential Buildings*. 2019, Vancouver, BC: BC Housing.
18. Motamedi, H., et al., *CFD modeling of airborne pathogen transmission of COVID-19 in confined spaces under different ventilation strategies.* Sustainable Cities and Society, 2022. **76**: p. 103397.
19. Chao, C.Y.H., et al., *Characterization of expiration air jets and droplet size distributions immediately at the mouth opening.* Journal of aerosol science, 2009. **40**(2): p. 122-133.
20. Fluent, A., *Fluent 15 users guide.* Lebanon, USA, 2016.
21. Edwards, D.A., et al., *Exhaled aerosol increases with COVID-19 infection, age, and obesity.* Proceedings of the National Academy of Sciences, 2021. **118**(8): p. e2021830118.
22. Dai, H. and B. Zhao. *Association of the infection probability of COVID-19 with ventilation rates in confined spaces*. in *Building simulation*. 2020. Springer.